Cascaded Approach for Despeckling SAR Images

Satinder Pal Singh[1], Dr. Sukhjeet Kaur[2]
[1]Student of Master of Philosophy, [2]Associate Professor
[1] Department of Computer Science
[1]Punjabi University Patiala, Punjab, India

Abstract: While capturing SAR images, a special type of noise can degrade its quality by blurring the detail part of image and that noise is usually multiplicative speckle noise. The process of elimination of that speckle noise is called despeckling SAR images which helps to preserve details of image, after removing noise factor, like structures, edges, corners etc. In this paper, the combination of frost filter and bilateral filter is used. Initially, the Frost filter is applied on noisy SAR image and edge enhancement is performed on the output of frost filter. Furthermore, Haar wavelet is applied on output of frost filter and calculates the median of diagonal detailed part of the image. Calculate the standard deviation and sigmar value. Apply the bilateral filter on the output of frost filter. Calculate the method noise for restoring that part of noisy image which is unfiltered. At last perform the element-wise multiplication of output of the method noise and edge enhancement. The quality of image is compared on the basis of performance measures like PSNR, MSE, MSSIM and UIQI. The performance is compared with all other existing filters and results show that the proposed method has brilliant performance.

***Index Terms* - Despeckling, Frost filter, Bilateral filter, Haar wavelet and SAR images.**

1. INTRODUCTION

Remote sensing means the activities of recording or observing or sensing electromagnetic energy reflected back by an object or event or target which are at faraway places. The remote sensing is divided into two types i.e. passive and active remote sensing. A passive sensor system always requires an external energy source which is mostly sun and active sensor has its own energy source or illumination. . SAR has been commonly used for Earth remote sensing for more than 30 years. . Synthetic aperture means the total distance traversed by the antenna. The total distance traversed by the signal is twice the distance travelled between the radar and the object, as the signal first travels from the sensor (radar) to the target object and then receiving back signal from that object to the radar after reflecting back to radar. It is a kind of high-resolution radar which is capable of creating or maintaining the data of hundreds of megabits of per second which allows high speed of processing as well as fast image acquisition process. SAR uses its own rays for capturing the images. It also uses microwave spectrum as well as multi-frequency.SAR is used to create 2-D or 3-D images of objects or events, such as building. It also provides 4-D mapping (space and time), it has also the capability of penetrating through deep shallow of the earth surface or brushwood. SAR is usually used for moving platform, like aircraft or spacecraft.

2. SPECKLE NOISE MODEL

In case of SAR imaging speckle noise is occur due to coherent nature. "Speckle noise" is a particular type of noise which has specific distribution function. Radar waves can interacts destructively or constructively to generate dark and light pixels called speckle noise. It is commonly recognized in radar sensor systems, but it may be present in any kind of coherent radiation utilizing the remotely sensed image. Speckle noise is supposed to be multiplicative in nature and it must be checked before the final data has to be saved otherwise the noise can degrades the quality image. It is not the similar to additive white Gaussian noise, Poisson noise, salt and pepper noise, etc.

Speckle noise in SAR images is considered as multiplicative noise; therefore the resultant or final signal is the product of original noise and speckle signal. Let us consider I (x, y) is the distorted or corrupted pixel of an observed target image and S (x, y) is the noise-free pixel of image which is to be recovered. According to this noise model,

$$I(x, y) = S(x, y) * \eta(x, y)$$

$\eta(x, y)$ is the multiplicative noise.

One common method to check the multiplicative noise is to transform the multiplicative model into an additive model, and after that apply each and everything you know very well from the additive noise model reduction field. You can perform this task easily by taking the logarithm of that signal, then filtering and at last the inverse log transformation.

$$\text{Log}(I(x, y)) = \log(S(x, y) * \eta(x, y))$$
$$= \log(S(x, y)) + \log(\eta(x, y))$$

There are mainly two types of speckle noise. Those are

- Laser speckle
- Dynamic speckle

Laser speckle is a problematic effect which is caused by the interference of the light scattered or distributed from adjacent points of any given rough object surface and leads to a random distribution of intensity. A laser speckle pattern is a pattern of intensity which is formed by the mutual interference of a group of wave-fronts. Speckle patterns generally present in diffuse (distributed) reflections or rays of monochromatic light like laser light. When you have the illuminated surface that produces the speckle effect presents (shows) some kind of activity i.e. with time, the speckle pattern changes. This phenomenon of effect is known as dynamic speckle or sometimes called bio-speckle.

3. GENERAL SPECKLE DENOISING TECHNIQUES:

SAR images are mainly altered by multiplicative noise as compared to the additive noise. The multiplicative noise present in SAR image is called speckle noise. This noise creates difficulties in various processes, like analyzing, interpretation, classification and detection of the SAR images. Consequently, you need a pre-processing step in speckled SAR image before its usage.

- **Lee filter**

The Lee filters calculates the linear combination of the intensity of the centre pixel in a window of filter by calculating the average or mean intensity of the window for eliminating the speckle noise.

$$\hat{R}\ (t) = I\ (t) * W\ (t) + \bar{I}\ (t) \times [1\text{-}W\ (t)],$$

Where $\hat{R}$ (t) is the de-noised or noiseless image, I (t) is the corrupted image with speckle noise and $\bar{I}\ (t)$ is the average intensity of an image within the given filter window. W (t) is the weighted coefficient which is determined as:

$$W(t) = 1 - \frac{C_u^2}{C_I^2(t)}$$

Here c_I (t) and c_u are the variation in the coefficients of speckle u (t) and the image I(t) respectively:

$$c_u = \frac{\sigma_u}{\bar{u}},\ c_I\ (t) = \frac{\sigma_{I(t)}}{\bar{I}(t)}$$

- **Median Filter**

The median filter is a spatial non-linear filter. In this filter the median value of neighbours of the window is calculated and that value is substituted at the centre of window to reduce the speckle noise. This filter works on the bases of the formula given below:

$$\hat{f}(x\ y) = \underset{(s,t)\in S_{xy}}{median}\ \{g(s,t)\}$$

Where g(s, t) is the original image, S_{xy} represent the coordinates of rectangular window of an image. This filter normally removes short duration or impulse noise, but not well suited in removing speckle noise.

- **Mean Filter**

Mean filter is a kind of simple filter. It is a low pass filter that not only smoothen the image but also blur the edges as well as fine details of the image. The working of this filter includes the calculation of the mean value of the neighbour pixels in the filter window. Then the calculated mean is substituted on the place of vale of the centre pixel of the window. This filter is implemented by using the formula given below:

$$\hat{f}(x,y) = \frac{1}{m.n} \sum_{(s,t)\in S_{xy}} g(s,t)$$

Where m.n is windows size of kernel, g(s,t) is the given original image, S_{xy} represents the coordinates of rectangular windows.

- **Frost Filter**

The Frost filter is a type of adaptive filter and is also exponentially weighted averaging filter which is determined by the coefficient of variation. The coefficient of variation is the ratio of the local mean to the local standard deviation of the given degraded image. This filter is implemented with the formula shown below:

$$DN = \sum_{n*n} k\alpha e^{-\alpha|t|}$$

Where k is constant of normalization, $|t| = |X - X0| + |Y - Y0|$, n is the size of moving window, α is calculated as $(4/n\sigma'2).(\sigma 2/\bar{I}2)$, σ is local variance, $\bar{I}$ is local mean, σ' is coefficient of variation of an image.

- **Kuan Filter**

The Kuan filter converts the multiplicative noise model into the additive noise model which is signal dependent and after transforming, the MMSE (i.e. minimum mean square error) procedure is applied. Final equation of this filter is similar to the equation of Lee filter, but the W(t) (weight factor) is different:

$$W(t) = \frac{1 - \frac{C_u^2}{C_I^2(t)}}{1 + C_u^2}$$

- **Improved Lee Filter**

The improved Lee filter assumes that the image areas are usually classified into one of three classes' type. First class includes all the homogenous areas in which the speckle noise is overcame by using simple low pass filter. Second class consists of all the heterogeneous areas; Lee filter equation is used for de-noising the speckle. Finally, the third class includes all isolated points, edges and other necessary features of an image with high variance. For third class, this filter recognizes or preserves original pixels from the observed image. These three classes can be written as:

$$\hat{R}\ (t) = \begin{cases} \bar{I}(t) & C_I(t) \le C_u \\ \bar{I}(t) & C_I(t) > C_{max}, \\ I(t).W(t) + \bar{I}(t).W'(t) & otherwise \end{cases}$$

$$W(t)=\exp\left(\frac{-K.[C_I(t)-C_u]}{C_{max}-C_I(t)}\right)$$

- **Wavelet Based De-Noising**

Speckle noise is a component of high-frequency in the target image and so naturally it affects the certain coefficients of the wavelet. So the speckle noise can be eliminated by modifying of appropriate coefficients of the wavelet. In general, the process starts with calculating the DWT and after calculation, the coefficients of wavelet are modified or thresholded and at the end, the image is regenerated or reconstructed with the help of IDWT. The best thresholding methods are soft and hard thresholding are.

Hard thresholding sets the value of all coefficients equal to zero when the coefficient lies in between $-x_{thr}$ and x_{thr} and remains unchanged when greater than x_{thr} according to the equation:

$$x' = \begin{cases} x & for|x| > |x_{thr}| \\ 0 & for -x_{thr} \le x \le x_{thr} \end{cases}$$

In Soft thresholding method, if the value of coefficient is greater than threshold then subtract that threshold value from the value of any coefficient which is greater than the threshold. If the value of any coefficient is less than threshold then add that threshold value to value of any coefficient that is smaller than the threshold and remains zero if the value of coefficient is in between $-x_{thr}$ and x_{thr}.

$$x' = \begin{cases} x - x_{thr} & for\ x > x_{thr} \\ 0 & -x_{thr} \le x \le x_{thr} \\ x + x_{thr} & for\ x < -x_{thr} \end{cases}$$

- **Wiener Filter**

Wiener filter is developed mainly for removal or elimination of the additional Gaussian noise, so due to this reason it is not possible to use this filter directly for the speckle de-noising. It decreases the MSE between the desired process and the estimated or assumed random process. The method considers the noise and images as random variables, and the main objective of this filter is to discover the estimated value of $\hat{f}$ of the uncorrupted or faultless image f so that the MSE (mean square error) in between them is lower or minimized. This measure of error is given by

$$e^2 = E\{(f-\hat{f})\}$$

Where E{.} is the expected or assumed value of argument

$$\hat{F}(u,v)=\left[\frac{H^*(u,v)S_f(u,v)}{S_f(u,v)|H(u,v)|^2+S_\eta(u,v)}\right]G(u,v)$$

H(u,v) is degradation function

$H^*(u,v)$ is the complex conjugate of H(u,v)

$|H(u,v)|^2 = H^*(u,v)\ H(u,v)$

$S_\eta(u,v)=|N(u,v)|^2$ is the power spectrum of noise

$S_f(u,v)=|F(u,v)^2|$ is the power spectrum of faultless or un-degraded image

- **Speckle Reduction Anisotropic Diffusion (SRAD)**

SRAD method was custom-made directly for radar imaging and the ultrasound applications. It uses instantaneous which is the function of magnitude, local gradient and Laplacian operators. Yongjian et al. makes allegation that SRAD method is better than the classical anisotropic reduction method at that time when the image is distorted by speckle noise. This method is based on PDE (partial different equation) that includes the image gradient, image intensity and Laplacian.

4. PROPOSED METHODOLOGY

The proposed method works on the basis of frost and bilateral filter. The whole algorithm is given as under:

Input: Speckled SAR image

Output: Despeckled SAR image

1 Apply Frost filter on Input Image and its output is denoted as F_{output}.

2 Apply the Edge enhancement on F_{output}, and get E_{output}.

3 Apply Haar wavelet on F_{output}.

3.1 Calculate the median of the diagonal detailed part of the image using the formula:

$$y[m,n] = median\ \{\ x[i,j],\ (i,j)\ \varepsilon\ W\}$$

where W is neighbourhood mask decided by user and it is centred around [m,n].

3.2 Calculate the standard deviation using formula:

$$SD = [median(|x(m,n)|) / 0.6745]$$

3.3 Calculate the value of sigmar using the formula given below:

Sigmar = multi_factor_sigmar * SD

3.4 Apply the Bilateral filter on F_{output} by using the sigmar, sigmas and ksize value. Output image is B_{output}

4 Apply method noise

(a) Calculate S by Subtracting B_{output} from F_{output} get S, as $S= F_{output} - B_{output}$.

(b) Apply Step-3 on S and resultant is E.

(c) Add S and E to get G, as G=S+E.

5 Apply Element-wise multiplication on E_{output} and G to get Final= E_{output} .* G

5. EXPERIMENTAL RESULTS

To conduct the experiment, I have proposed a method which uses Frost filter at initial stage. The size of mask for Frost filter is 3*3. On the other side, edge enhancement has been conducted on the output of Frost filter. The Haar Wavelet is also applied on the Frost filter's output and it segmented the image into four parts i.e. approximation, horizontal, vertical and diagonal part. In my experiment I have considered the diagonal part. The values of sigmas, ksize and multi_factor_sigmar are set as 0.5, 3 and 3 respectively. The visual quality of all filters goes on decreasing when the noise variance is increased but the visual quality of output image of proposed method is still good to identify the object in the image.

The experimental results are shown under in figures. The fig 5.1 and 5.2 shows the results of one SAR image at different noise variance i.e. 0.004 and 0.01. The fig 5.3 and 5.4 shows the results at same noise variance. In fig 5.5 and 5.6, the behavior of different filters is shown. Furthermore fig 5.7 and 5.8 displays the output of different filters at different NV.

Similarly, the values of different performance measures are shown in the form of tables. In table 5.1, the value of PSNR is shown and the MSE value of different filters is shown in table 5.2 and the value of MSSIM is shown in table 5.3 and table 5.4 displays the value of UIQI. The highest values of PSNR are bolded whereas the lost values in MSE table are also bolded. In most of the cases, the proposed method works well.

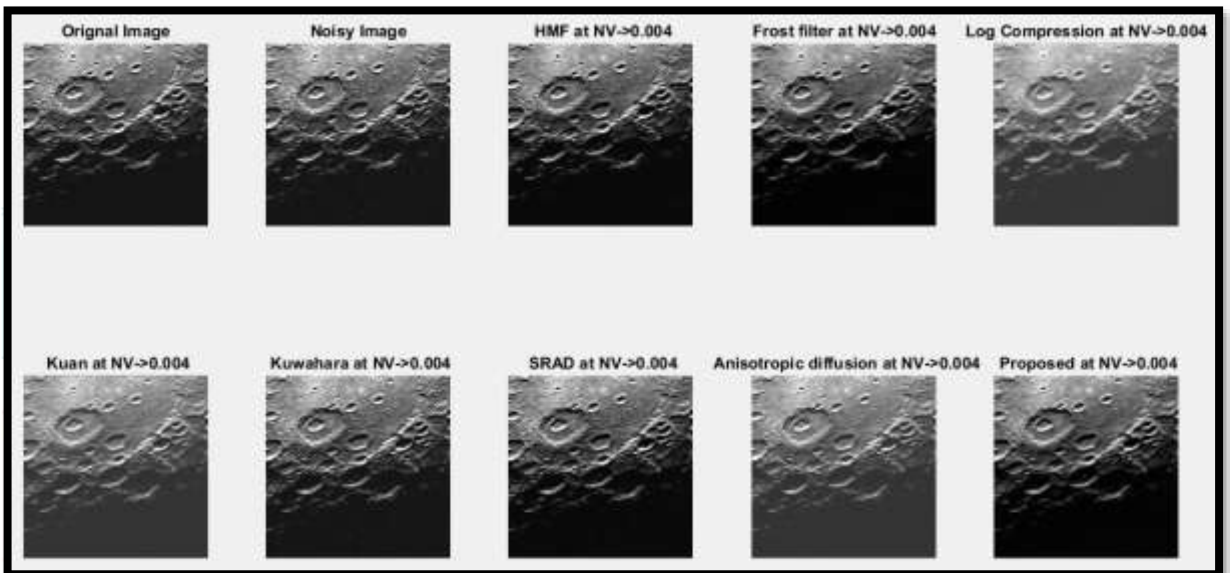

Fig. 5.1 SAR-1 results of different filters at noise variance 0.004

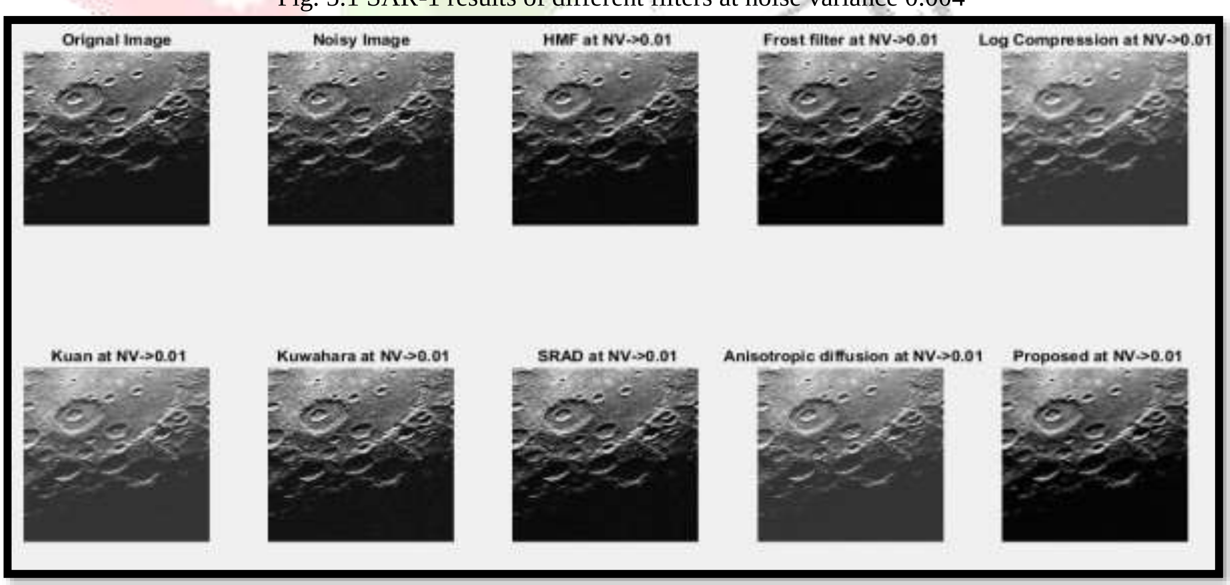

Fig. 5.2 SAR-1 results of different filters at NV 0.01

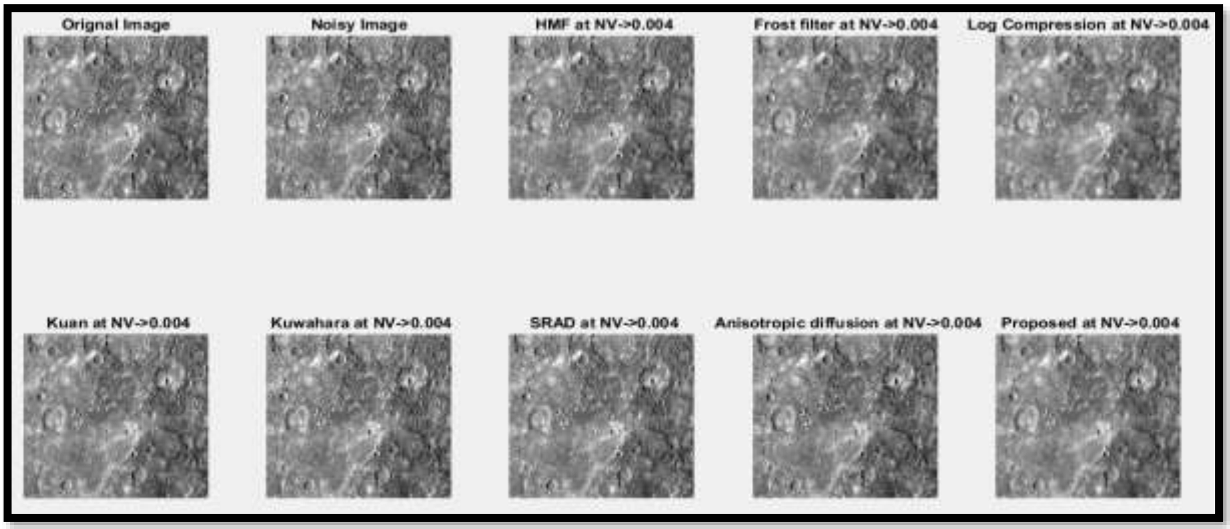

Fig. 5.3 SAR-2 results of different filters at noise variance 0.004

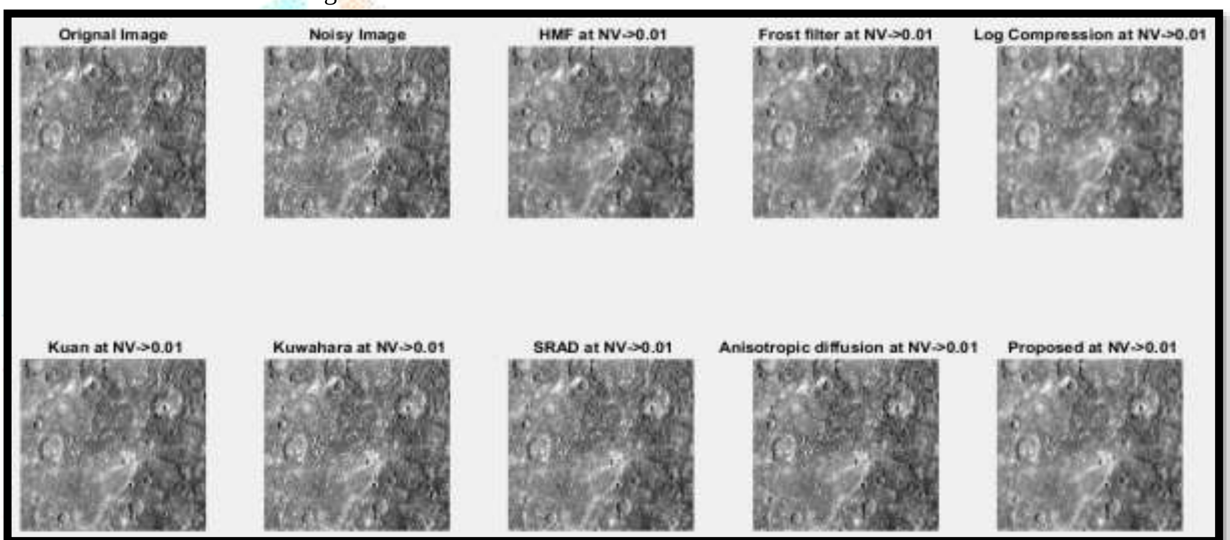

Fig. 5.4 SAR-2 results of different filters at noise variance 0.01

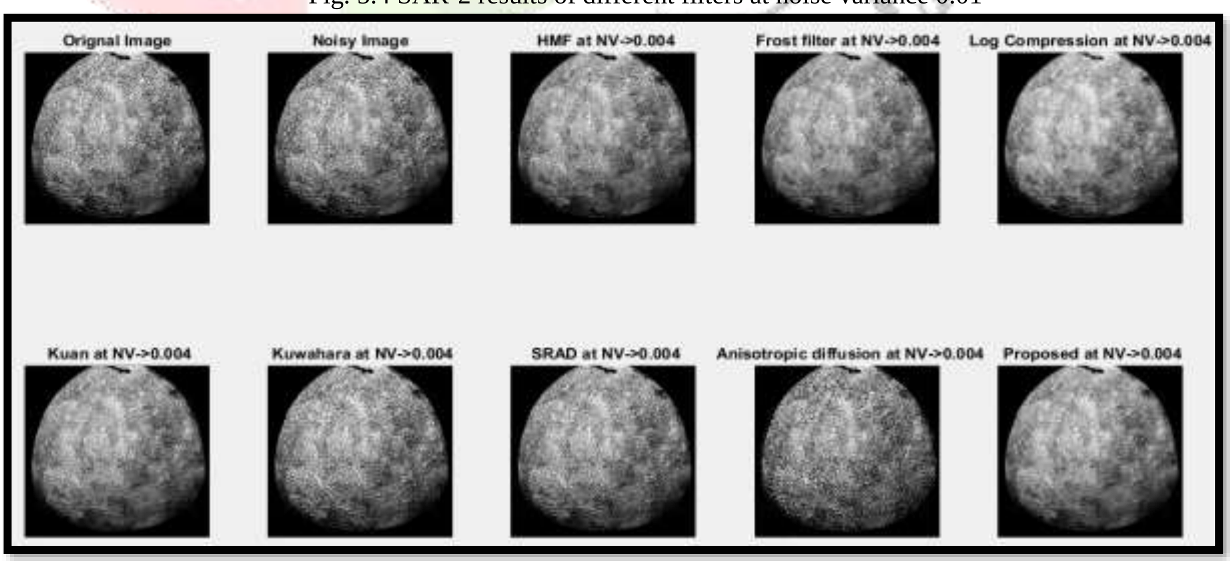

Fig. 5.5 SAR-3 results of different filters at noise variance 0.004

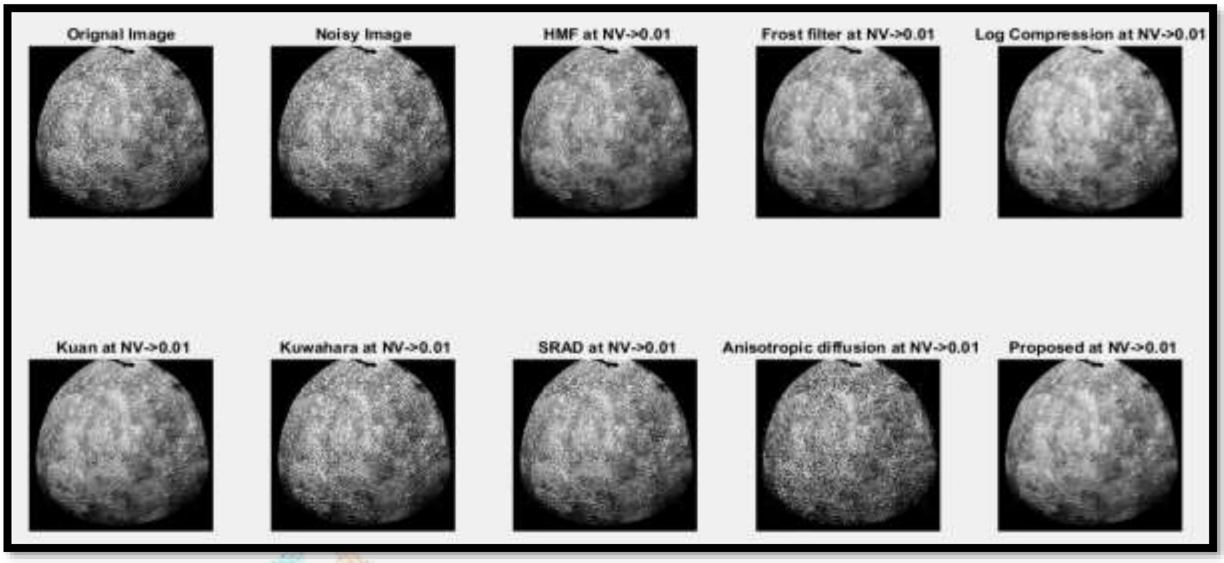

Fig. 5.6 SAR-3 results of different filters at noise variance 0.01

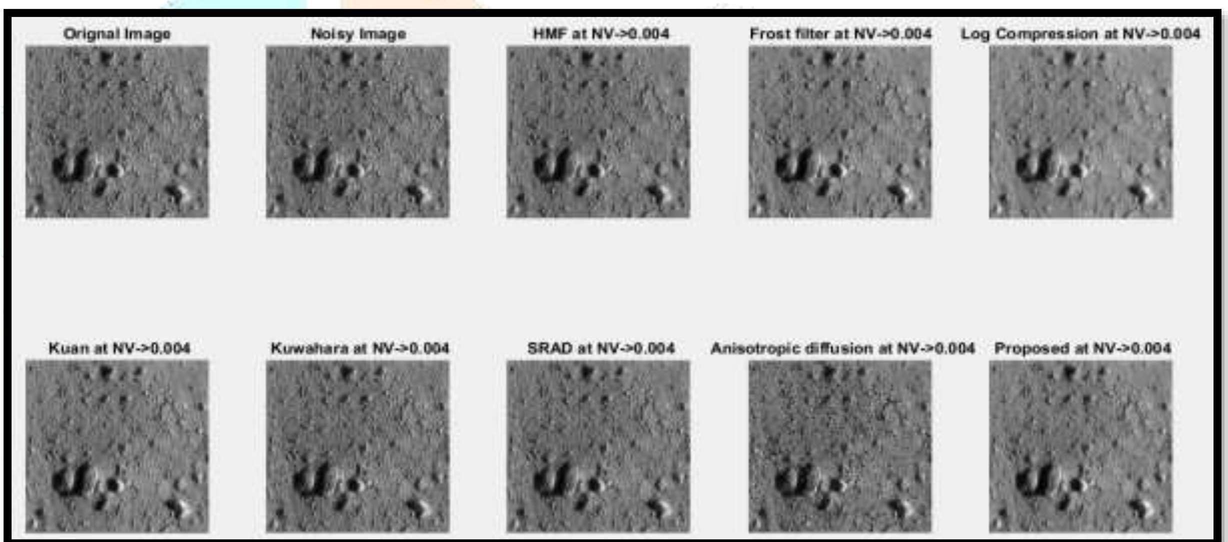

Fig. 5.7 SAR-4 results of different filters at noise variance 0.004

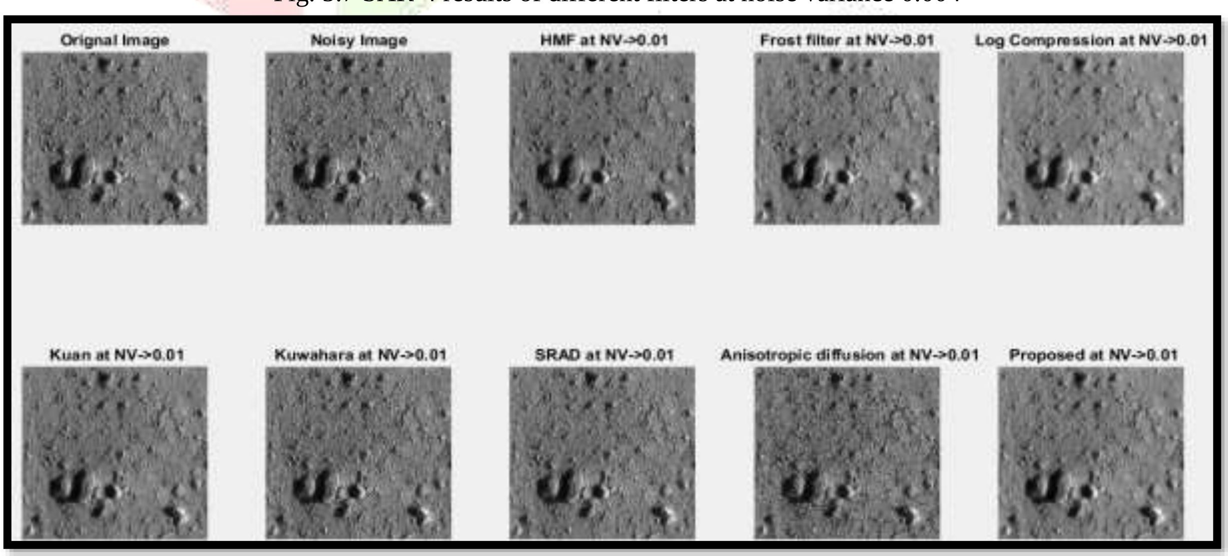

Fig. 5.8 SAR-4 results of different filters at noise variance 0.01

Table 5.1 PSNR table of despeckled different SAR images

PSNR Table							
Image	**Noise Variance**	**0.004**	**0.01**	**0.02**	**0.03**	**0.04**	**0.05**
SAR-1	HMF	31.0255	29.2890	27.5286	26.3348	25.4497	24.7325
	Frost	27.0342	26.8891	26.7104	26.5324	26.3699	26.1608
	Log Com.	23.9408	23.8021	23.5954	23.3997	23.1813	22.9752
	Kuan	28.7740	28.3289	27.7329	27.0809	26.8734	26.3250
	Kuwahara	31.6601	27.7047	24.7321	23.0092	21.7852	20.8581
	SRAD	32.5502	29.0241	26.1981	24.5014	23.2891	22.3522
	Ani. Diff.	27.8642	25.9549	22.6163	19.3955	17.3149	16.0048
	Proposed	**33.2608**	**30.7433**	**29.7683**	**29.0065**	**28.4035**	**27.8461**
SAR-2	HMF	29.1800	27.5341	25.7883	24.6347	23.7406	23.0089
	Frost	25.7505	25.6682	25.7939	25.3491	25.2046	25.0292
	Log Com.	22.7780	22.7244	22.6060	22.4905	22.3377	22.1916
	Kuan	28.4579	27.82221	27.0775	26.3670	25.9310	25.3670
	Kuwahara	29.6181	25.6735	22.6667	20.9386	19.6994	18.7661
	SRAD	30.6817	27.1165	24.2184	22.5108	21.2691	20.3245
	Anisotropic Diffusion	22.9097	21.6214	19.2028	16.6573	14.9185	13.9608
	Proposed	**31.7737**	**27.8874**	**27.0853**	**26.4150**	**26.0244**	**25.4797**
SAR-3	HMF	22.9936	22.6963	22.2534	21.8239	21.4745	21.1430
	Frost	20.5206	20.5073	20.4885	20.4570	20.4281	20.3978
	Log Com.	19.2868	19.2424	19.1493	19.0816	18.9966	18.9272
	Kuan	22.2015	22.0953	21.9277	21.7648	21.6094	21.4558
	Kuwahara	31.0445	27.1241	24.1987	22.4782	21.3136	20.3837
	SRAD	30.2241	27.5440	25.1124	23.5448	22.4628	21.5718
	Ani. Diff.	16.3277	15.8908	15.6165	14.8385	14.5268	14.3657
	Proposed	**31.4368**	**27.5553**	**25.5578**	**24.1561**	**23.2184**	**22.4475**
SAR-4	HMF	29.4703	27.9124	26.3629	25.2661	24.4448	23.7862
	Frost	24.7341	24.7046	24.6634	24.6171	24.5507	24.5002
	Log Com.	22.7136	22.6823	22.6265	22.5488	22.4767	22.3536
	Kuan	27.6943	27.3332	**26.9310**	26.4906	26.0528	25.6301
	Kuwahara	31.0156	27.0553	24.0570	22.2909	21.0516	20.0812
	SRAD	31.8420	28.3830	25.5530	23.8285	22.5922	21.6162
	Ani. Diff.	19.7011	18.8632	17.4568	16.0649	15.0139	14.3667
	Proposed	**32.5180**	**29.7654**	26.9131	**26.4957**	**26.0952**	**25.6827**

Table 5.2 MSE table of despeckled different SAR images

MSE Table							
Image	**Noise Variance**	**0.004**	**0.01**	**0.02**	**0.03**	**0.04**	**0.05**
SAR-1	HMF	51.3490	76.5919	114.8749	151.2182	185.4001	218.6920
	Frost	128.7251	133.0964	138.6881	144.4898	149.9996	157.3995
	Log Com.	262.4202	270.9392	284.1456	297.2412	312.5732	327.7637
	Kuan	86.2348	95.5409	109.5955	127.3468	133.5796	151.5569
	Kuwahara	44.3676	110.3098	218.7133	325.2099	431.0866	533.6658
	SRAD	36.1461	81.4092	156.0511	230.6441	304.9106	378.3170
	Ani. Diff.	106.3318	165.0400	355.9966	747.3582	1.2067e+03	1.6315e+03
	Proposed	**30.6902**	**54.7965**	**68.5890**	**81.7399**	**93.9130**	**106.7744**
SAR-2	HMF	78.5385	114.7274	171.4945	223.6704	274.8038	325.2266
	Frost	172.9925	176.3033	183.5235	189.7470	196.1632	204.2498
	Log Com.	342.9925	347.2517	356.8426	366.4616	379.5879	392.5705
	Kuan	92.7454	104.7226	127.4476	150.0991	165.9529	188.9637
	Kuwahara	71.0027	176.0869	351.8888	523.8683	696.8559	863.9196
	SRAD	55.5792	126.3079	246.1744	364.7583	485.4766	603.4299

	Ani. Diff.	332.7437	447.6529	781.2749	1.4039e+03	2.0952e+03	2.6122e+03
	Proposed	**43.2227**	**104.7655**	**127.2174**	**148.4512**	**162.4208**	**184.1254**
SAR-3	HMF	326.3756	349.5024	387.0249	427.2581	463.0540	499.7792
	Frost	576.7925	578.5581	581.0738	585.3092	589.2070	593.3345
	Log Com.	766.2969	774.1781	790.9503	803.3787	819.2648	832.4591
	Kuan	391.6767	401.3785	417.1683	433.1075	448.8870	465.0502
	Kuwahara	51.1246	126.0871	247.2942	367.4983	480.5337	595.2645
	SRAD	61.7546	114.4666	200.3720	287.4745	368.8102	452.7887
	Ani. Diff.	1.5146e+03	1.6749e+03	1.9118e+03	2.1342e+03	2.2930e+03	2.3796e+03
	Proposed	**46.7090**	**114.1704**	**180.8437**	**249.7303**	**309.9118**	**370.1059**
SAR-4	HMF	73.4592	105.1576	150.2408	193.4049	233.6686	271.9309
	Frost	218.6099	220.0984	222.1987	224.5804	228.0375	230.7079
	Log Com.	348.1167	350.6273	355.1636	361.5788	367.6333	378.2002
	Kuan	110.5739	120.1613	**131.8188**	145.8898	160.9922	177.8564
	Kuwahara	51.4659	128.0999	255.4948	383.6992	510.4107	638.2031
	SRAD	42.5480	94.3585	181.0412	269.2982	357.9806	448.1845
	Ani. Diff.	696.5832	844.8033	1.1679e+03	1.6091e+03	2.0497e+03	2.3791e+03
	Proposed	**36.4148**	**68.6339**	132.3650	**145.7177**	**159.7922**	**175.7163**

Table 5.3 MSSIM table of despeckled different SAR images

MSSIM Table							
Image	**Noise Variance**	**0.004**	**0.01**	**0.02**	**0.03**	**0.04**	**0.05**
SAR-1	HMF	0.9052	0.8533	0.7832	0.7286	0.6845	0.6486
	Frost	0.8235	0.8193	0.8127	0.8069	0.8015	0.7935
	Log Com.	0.7777	0.7351	0.6771	0.6317	0.5917	0.5600
	Kuan	0.9271	0.9076	0.8775	0.8508	0.8277	0.8051
	Kuwahara	0.8794	0.7604	0.6330	0.5486	0.4887	0.4427
	SRAD	0.9050	0.8099	0.6978	0.6173	0.5574	0.5099
	Ani. Diff.	0.8785	0.8194	0.6322	0.3865	0.2466	0.1815
	Proposed	**0.9343**	**0.9133**	**0.8870**	**0.8582**	**0.8394**	**0.8183**
SAR-2	HMF	0.8662	0.8064	0.7299	0.6758	0.6327	0.5945
	Frost	0.7173	0.7153	0.7093	0.7052	0.7001	0.6939
	Log Com.	0.6008	0.5983	0.5952	0.5935	0.5923	0.5889
	Kuan	0.8970	0.8750	0.8425	0.8151	0.7902	0.7661
	Kuwahara	0.8769	0.7571	0.6295	0.5464	0.4864	0.4395
	SRAD	0.8963	0.7971	0.6827	0.6035	0.5441	0.4963
	Ani. Diff.	0.7409	0.6352	0.4135	0.2436	0.1765	0.1541
	Proposed	**0.9221**	**0.8766**	**0.8428**	**0.8178**	**0.7953**	**0.7726**
SAR-3	HMF	0.7888	0.7763	0.7578	0.7402	0.7274	0.7149
	Frost	0.5838	0.5846	0.5862	0.5862	0.5862	0.5876
	Log Com.	0.5283	0.5270	0.5234	0.5213	0.5173	0.5154
	Kuan	0.7467	0.7422	0.7355	0.7282	0.7214	0.7152
	Kuwahara	0.9746	0.9315	0.8954	0.8565	0.8251	0.7963
	SRAD	0.9665	0.9325	0.9008	0.8668	0.8390	0.8130
	Ani. Diff.	0.4454	0.4173	0.4018	0.4024	0.4132	0.4251
	Proposed	**0.9750**	**0.9357**	**0.9044**	**0.8758**	**0.8528**	**0.8315**
SAR-4	HMF	0.8688	0.8152	0.7525	0.7030	0.6638	0.6320
	Frost	0.6046	0.6047	0.6060	0.6076	0.6067	0.6072
	Log Com.	0.5080	0.5079	0.5095	0.5104	0.5106	0.5114
	Kuan	0.8502	0.8355	**0.8149**	0.7924	0.7763	0.7602
	Kuwahara	0.9142	0.8219	0.7156	0.6389	0.5808	0.5345
	SRAD	0.9240	0.8489	0.7569	0.6871	0.6319	0.5871
	Ani. Diff.	0.4804	0.3800	0.2408	0.1727	0.1540	0.1558
	Proposed	**0.9360**	**0.8847**	0.8127	**0.7939**	**0.7765**	**0.7614**

Table 5.4 UIQI table of despeckled different SAR images

UIQI Table							
Image	**Noise Variance**	**0.004**	**0.01**	**0.02**	**0.03**	**0.04**	**0.05**
SAR-1	HMF	0.9988	0.9982	0.9971	0.9960	0.9950	0.9940
	Frost	0.9961	0.9960	0.9957	0.9954	0.9951	0.9948
	Log Com.	0.9882	0.9879	0.9872	0.9866	0.9859	0.9852
	Kuan	0.9986	0.9983	0.9977	0.9970	0.9965	0.9959
	Kuwahara	0.9994	0.9988	0.9977	0.9965	0.9953	0.9942
	SRAD	**0.9995**	**0.9989**	**0.9980**	0.9970	0.9962	0.9952
	Ani. Diff.	0.9975	0.9958	0.9920	0.9860	0.9792	0.9724
	Proposed	0.9993	0.9982	**0.9980**	**0.9974**	**0.9966**	**0.9960**
SAR-2	HMF	0.9980	0.9974	0.9964	0.9957	0.9944	0.9935
	Frost	0.9941	0.9939	0.9937	0.9932	0.9936	0.9928
	Log Com.	0.9853	0.9848	0.9842	0.9836	0.9806	0.9821
	Kuan	0.9978	0.9976	0.9967	0.9962	**0.9969**	0.9951
	Kuwahara	**0.9995**	**0.9989**	0.9977	0.9965	0.9955	0.9942
	SRAD	0.9993	0.9988	**0.9978**	0.9970	0.9961	0.9952
	Ani. Diff.	0.9936	0.9920	0.9881	0.9821	0.9756	0.9703
	Proposed	0.9992	0.9974	0.9967	**0.9970**	0.9954	**0.9953**
SAR-3	HMF	0.9770	0.9762	0.9735	0.9739	0.9741	0.9716
	Frost	0.9573	0.9664	0.9618	0.9670	0.9645	0.9675
	Log Com.	0.9601	0.9627	0.9614	0.9587	0.9529	0.9601
	Kuan	0.9644	0.9617	0.9610	0.9614	0.9643	0.9600
	Kuwahara	**0.9989**	**0.9978**	**0.9953**	**0.9925**	**0.9907**	0.9904
	SRAD	0.9974	0.9963	0.9939	0.9899	0.9894	0.9883
	Ani. Diff.	0.9087	0.9130	0.9046	0.9046	0.9082	0.9040
	Proposed	0.9943	0.9914	0.9044	0.9871	0.9864	**0.9905**
SAR-4	HMF	0.9971	0.9968	0.9950	0.9945	0.9920	0.9905
	Frost	0.9904	0.9910	0.9902	0.9900	0.9893	0.9892
	Log Com.	0.9809	0.9802	0.9813	0.9810	0.9775	0.9801
	Kuan	0.9961	0.9960	0.9952	0.9944	0.9927	0.9927
	Kuwahara	**0.9992**	0.9964	0.9948	0.9940	**0.9951**	0.9934
	SRAD	0.9990	**0.9993**	0.9971	0.9945	0.9948	**0.9949**
	Ani. Diff.	0.9830	0.9812	0.9792	0.9749	0.9723	0.9733
	Proposed	0.9989	0.9981	**0.9972**	**0.9946**	0.9937	0.9934

6. OVERALL PERFORMANCE OF DIFFERENT FILTERS

The performance of different despeckling methods is shown below. Different performance measures are shown in different figure. Numbers of images are considered to compare filters. The database of 35 images are considered to conduct the experiment and the value of parameter measures all filters is displayed and it is proved that the proposed method has best among all. In fig. 6.1, the PSNR value of different filters is displayed. The fig. 6.2 displays the MSE value and the fig 6.3 represents the MSSIM value whereas in fig 6.4, the UIQI value of different filters is displayed.

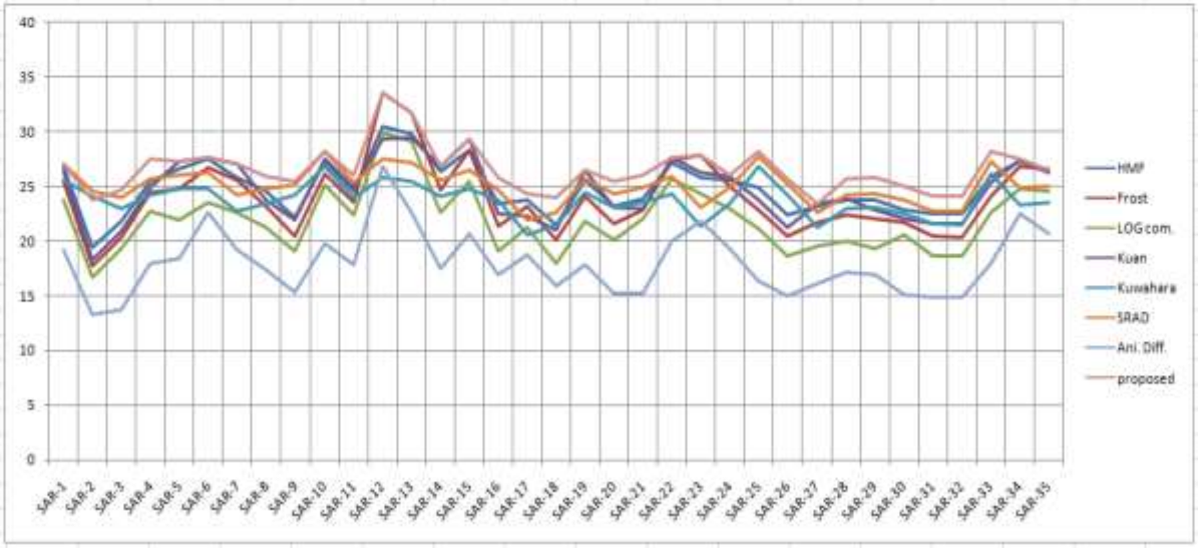

Fig 6.1 PSNR value of different filters at NV 0.02

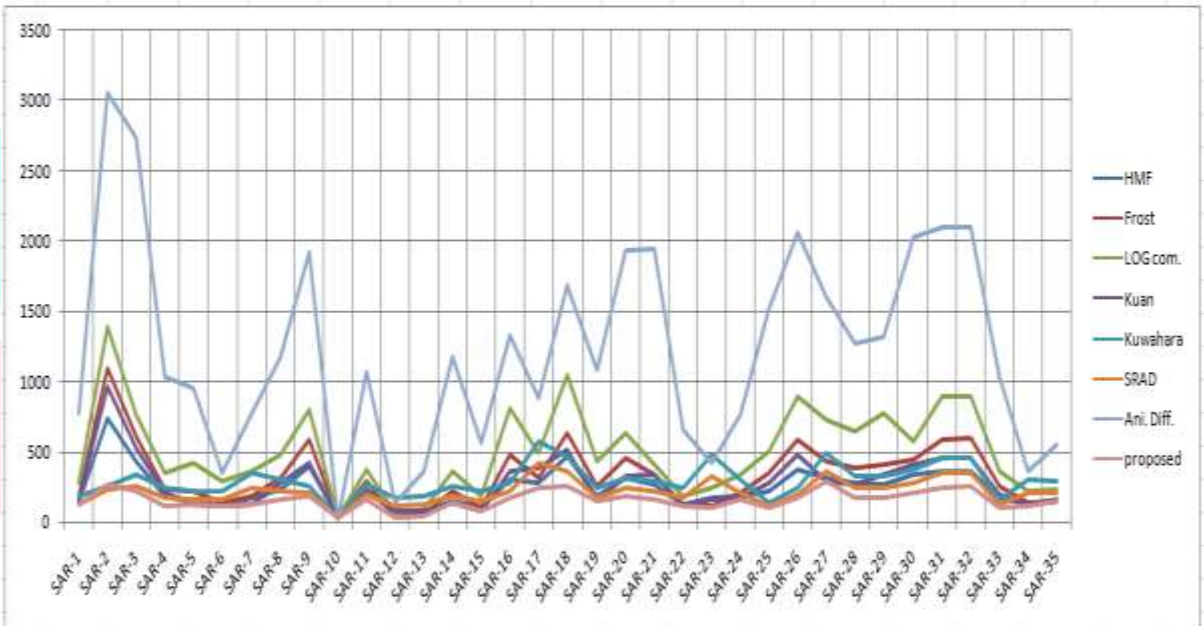

Fig. 6.2 MSE values of different filters at NV 0.02

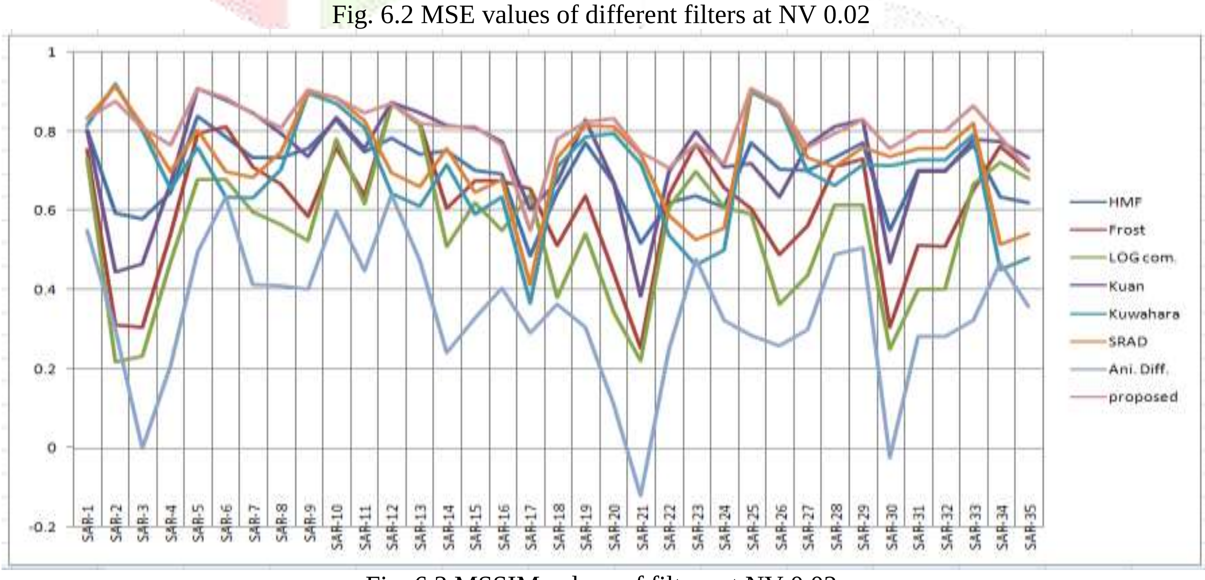

Fig. 6.3 MSSIM values of filters at NV 0.02

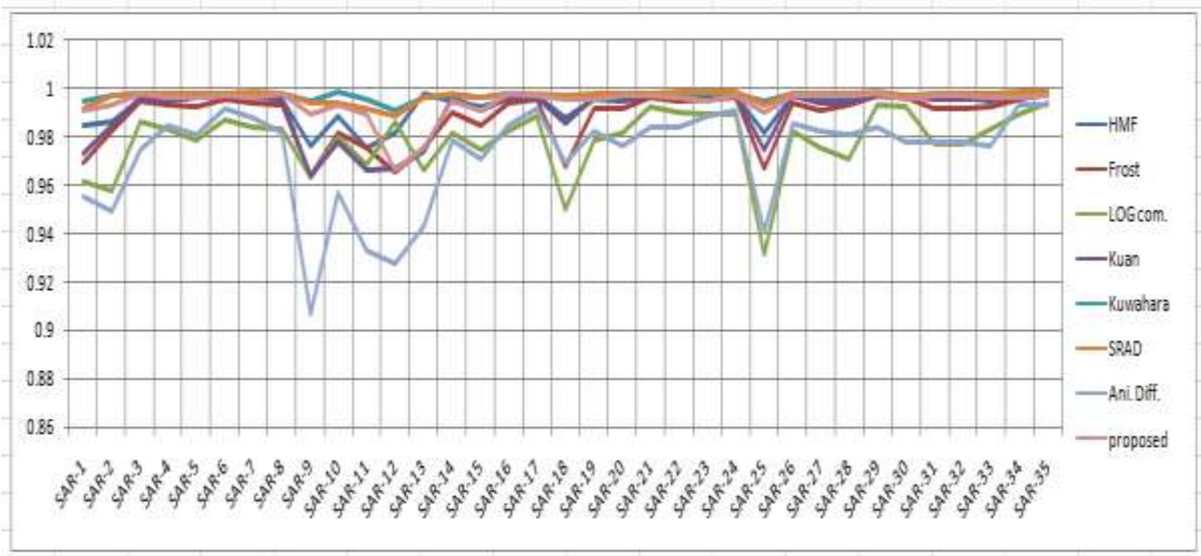

Fig. 6.4 Graphical representation of UIQI value

7. CONCLUSION

Various filters are available for denoising the SAR image. Those filters are Lee filter, Mean filter, Median filter, Frost filter, Kuan filter, Improved Lee filter, Wavelet based de-noising, Wiener filter, Speckle Reduction Anisotropic Diffusion, Gamma-MAP Filter, etc. The comparison of different filters can be made on the basis of different performance measures i.e. PSNR, MSE, SSIM and UIQI. I have proposed a method for despeckling the noisy SAR image. The procedure of proposed approach is: initially the noisy SAR image is taken as input. Apply the Frost filter on input noisy SAR image. Haar wavelet as well as edge enhancement is applied on the image produced by the Frost filter. The diagonal part is selected for further processing. After applying Haar, the median of the diagonal part of the image is calculated and by using that median, the standard deviation is calculated and at last the value of sigmer is calculated by using standard deviation. Then bilateral filter is applied on the output image generated with the help of Frost filter along with sigmar, sigmas and ksize value. Method noise is applied and at last the element-wise multiplication of output of method noise and edge enhancement has taken place. In most of the cases, the output image of proposed method has highest PSNR value and best visual quality as compared to all other denoising filters. In future we will try to enhance the features near the edges where the proposed method not works well sometimes and also enhance the quality in homomorphic regions.

8. REFERENCES

[1] Wensen Fenga, Yunjin Chenb, "Speckle Reduction with Trained Nonlinear Diffusion Filtering", Journal of Mathematical Imaging and Vision, February 27, 2017.

[2] Prabhishek singh, raj shree, "a new Homomorphic and method noise thresholding based despeckling of SAR image using anisotropic diffusion", journal of king saud university- computer and information sciences, Elsevier, 2017.

[3] D. Hazarika, V. K. Nath and M. Bhuyan, "Speckle Removal From SAR Images in the Lapped Transform Domain Using Adaptive Threshold Based on Despeckling Evaluation Indexes", 4th International Conference on Recent Trends in Computer Science & Engineering, Elsevier, Procedia Computer Science 87: 148 – 155, 2016.

[4] Vikrant Bhateja, Aditi Sharma, Abhishek Tripathi, Suresh Chandra Satapathy, and Dac-Nhuong Le, "An Optimized Anisotropic Diffusion Approach for Despeckling of SAR Images", Springer Nature Singapore, CSI 2016, CCIS 679, pp. 134–140, 2016.

[5] Alfredo E. Palacios Enr´ıquez and Volodymyr Ponomaryov, "Image Denoising using Block Matching and Discrete Cosine Transform with Edge Restoring", IEEE Conference Proceedings. Conielecomp 2016, February 24-26, 2016.

[6] M. A. Amritkar, K. J. Mahajan, "Comparative Approach of Dct And Dwt For Sar Image Fusion", International Journal Of Advances In Electronics and Computer Science, ISSN: 2393-2835 Volume-3, Issue-1, Jan. 2016.

[7] Bodh Raj, Arun Sharma, Kapil Kapoor, Divya Jyoti, "A Novel approach for the Reduction of Noise", International Journal of Advance Research , Ideas and Innovations in Technology, ISSN: 2454-132X, Volume2, Issue3, 2016.

[8] D. Hazarika, V. K. Nath and M. Bhuyan, "Speckle Removal From SAR Images in the Lapped Transform Domain Using Adaptive Threshold Based on Despeckling Evaluation Indexes", 4th International Conference on Recent Trends in Computer Science & Engineering, Elsevier, Procedia Computer Science 87: 148 – 155, 2016.

[9] Abhishek Tripathi and vikrant bhateja, "kuan modified anisotropic diffusion approach for speckle filtering", Elsevier, Pp. 537-545, 2016.

[10] Vikrant bhateja, anubhav tripathi, anurag gupta, aime lay-Ekuakille, "speckle suppression in SAR images employing modified anisotropic diffusion filtering in wavelet domain for environment monitoring", Elsevier, .easurement 74: 246-254, 2015.

[11] Li Gun, Li Cuihua, Zhu Yingpan & Huang Feijiang, "An improved speckle-reduction algorithm for SAR images based on anisotropic diffusion", Springer Science+Business Media New York 2015, august 2015.

[12] Premal B. Nirpal, "Image Compression using Discrete Cosine Transform, Block Truncation Coding and Gaussian Pyramidal Approach", International Journal of Computer Sciences and Engineering, Volume-3, Issue-4, E-ISSN: 2347-2693, April 30, 2015.

[13] Simranjit Kour, Bikrampal Kaur, "Design of Hybrid Filter with Wavelet denoising and Anisotropic Diffusion Filter for Image Despeckling", International Journal of Computer Applications (0975 – 8887) Volume 115 – No. 19, April 2015.

[14] Xiaoshuang Ma, Huanfeng Shen, Liangpei Zhang, Jie Yang, and Hongyan Zhang, "Adaptive Anisotropic Diffusion Method for Polarimetric SAR Speckle Filtering", IEEE Journal Of Selected Topics In Applied Earth Observations And Remote Sensing, Vol. 8, No. 3, Pp. 1042-1050, March 2015.

[15] Tae Hee Kim and Ram M. Narayanan, "Compressive Sensing Based Image Reconstruction for Synthetic Aperture Radar Using Discrete Cosine Transform and Noiselets", IEEE, 2015.

[16] MuraliMohanBabu. Y, Subramanyam. M. V, GiriPrasad. M. N, "A modified BM3D algorithm for SAR image despeckling", 4thInternational Conference on Eco-friendly Computing and Communication Systems, Elsevier, Procedia Computer Science 70: 69 – 75, 2015.

[17] Mehmet Ali SOYTURK, Alper BAS¸TURK, Mehmet Emin YUKSEL, "A novel fuzzy filter for speckle noise removal", Turkish Journal of Electrical Engineering & Computer Sciences 22: 1367 – 1381, 2014.

[18] Luis Gómez, Cristian Munteanu, Julio Berlles, Marta Mejail, "Evolutionary Expert-Supervised Despeckled SRAD filter design for SAR images", 2014.

[19] Lei zhu, xiaotian zhao and meihua gu, "SAR image despeckling using improved detail-preserving anisotropic diffusion", ELECTRONICS LETTERS Vol. 50 No. 15 pp. 1092–1093, 17th July 2014.

[20] L. Fabbrini, M. Greco, M. Messina and G. Pinelli, "Improved anisotropic diffusion filtering for SAR image despeckling", ELECTRONICS LETTERS Vol. 49 No. 10, 9th May 2013.

[21] Sheng Sun, Jinwen Tian, Zhusong Liu, Nian Cai, "Anisotropic diffusion for speckle filtering of polarimetric synthetic aperture radar imagery", Journal of Electronic Imaging 22(1), 013003, Jan–Mar 2013.

[22] B. K. Shreyamsha Kumar, "Image denoising based on gaussian/bilateral filter and its method noise thresholding", Springer-Verlag London Limited, 5 Sept. 2012.

[23] Ashkan Masoomi, Roozbeh Hamzehyan, and Najmeh Cheraghi Shirazi, "Speckle Reduction Approach for SAR Image in Satellite Communication", International Journal of Machine Learning and Computing, Vol. 2, No. 1, February 2012.

[24] Rajeshwari G.S., R Runa Simon, Sulochana R. and J. B. Bhattacharjee, "despeckling of SAR images using recursive filter based, model based and anisotropic diffusion based methods", Anale. Seria Informatică, Vol. X fasc. 2 – 2012.

[25] R. Sivakumar, M. K. Gayathri and D. Nedumaran, "Speckle Filtering of Ultrasound B-Scan Images - A Comparative Study of Single Scale Spatial Adaptive Filters, Multiscale Filter and Diffusion Filters", IACSIT International Journal of Engineering and Technology, Vol.2, No.6, ISSN: 1793-8236, December 2010.

[26] Yi Wang, Ruiqing Niu, Ke Wu, Xin Yu, "Wavelet-Based Multiscale Anisotropic Diffusion for Speckle Reduction and Edge Enhancement ",Multispectral Image Acquisition and Processing, ResearchGate, 2009.

[27] Somchai Easanuruk, Somsak Mitathal, Sathit Intajag, Sakreya Chitwong, "Speckle Reduction Using Fuzzy Morphological Anisotropic Diffusion", IEEE, 2005.

[28] Scott T. Acton, "Deconvolutional Speckle Reducing Anisotropic Diffusion", IEEE, 2005.

[29] Chen Xi, Wang Chao, Zhang Hong, Tang Yixian, "Anisotropic Diffusion Despeckling for High Resolution SAR Images", 25th ACRS 2004 Chiang Mai, Thailand, 2004.

[30] Yongjian Yu and Scott T. Acton, "Speckle Reducing Anisotropic Diffusion", IEEE Transactions on Image Processing, Vol. 11, No. 11, November 2002,

[31] Fatma A. Sakaya,Dong Wei, and Serkan Emek, "An Evaluation Of Sar Image Compression Techniques", IEEE, 1997.

[32] Francine Cattle, Pierre-Louis Lions, Jean-Michel Morel, and Tomeu Coll, "Image Selective Smoothing and Edge Detection by Nonlinear Diffusion", Siam J. Numer. Anal. Vol. 29 No. 1, Pp. 182-193, February 1992.

[33] Pietro Perona and Jitendra Malik, "Scale-Space And Edge Detection Using Anisotropic Diffusion", IEEE Transactions on Pattern Analysis And Machine Intelligence, Vol. 12. No. 7, Pp. 629-639, July 1990.